

High-Resolution *Plasmodium falciparum* Malaria Risk Mapping in Mutasa District, Zimbabwe: Implications for Regaining Control

Mufaro Kanyangarara,^{1*} Edmore Mamini,² Sungano Mharakurwa,² Shungu Munyati,² Lovemore Gwanzura,³ Tamaki Kobayashi,⁴ Timothy Shields,⁴ Luke C. Mullany,¹ Susan Mutambu,⁵ Peter R. Mason,² Frank C. Curriero,⁴ and William J. Moss⁴ for the Southern Africa International Centers of Excellence for Malaria Research

¹Department of International Health, Johns Hopkins Bloomberg School of Public Health, Johns Hopkins University, Baltimore, Maryland; ²Biomedical Research and Training Institute, Harare, Zimbabwe; ³Department of Medical Laboratory Sciences, College of Health Sciences, University of Zimbabwe, Harare, Zimbabwe; ⁴Department of Epidemiology, Johns Hopkins Bloomberg School of Public Health, Johns Hopkins University, Baltimore, Maryland; ⁵National Institute of Health Research, Harare, Zimbabwe

Abstract. In Zimbabwe, more than half of malaria cases are concentrated in Manicaland Province, where seasonal malaria epidemics occur despite intensified control strategies. The objectives of this study were to develop a prediction model based on environmental risk factors and obtain seasonal malaria risk maps for Mutasa District, one of the worst affected districts in Manicaland Province. From October 2012 to September 2015, 483 households were surveyed, and 104 individuals residing within 69 households had positive rapid diagnostic test results. Logistic regression was used to model the probability of household positivity as a function of the environmental covariates extracted from high-resolution remote sensing data sources. Model predictions and prediction standard errors were generated for the rainy and dry seasons. The resulting maps predicted elevated risk during the rainy season, particularly in low-lying areas bordering Mozambique. In contrast, the risk of malaria was low across the study area during the dry season with foci of malaria risk scattered along the northern and western peripheries of the study area. These findings underscore the need for strong cross-border malaria control initiatives to complement country-specific interventions.

INTRODUCTION

Since the 1950s, Zimbabwe dramatically reduced the national burden of malaria, largely through diagnosis and treatment and indoor residual spraying (IRS), and more recently, the distribution of insecticide-treated bed nets.¹ Despite this, malaria has reemerged as a public health problem in the past decade and this resurgence has been attributed to limited funding for control, drug resistance by *Plasmodium* parasites, and insecticide resistance by major Anopheline vectors.^{2–5} The reemergence of malaria in areas with previously successful control poses a challenge to the sustainability of gains made in reducing malaria and current efforts to reduce the burden of malaria to achieve elimination. More than half of malaria cases reported in Zimbabwe in recent years occurred in Manicaland Province, where malaria transmission continues despite intensified control strategies.^{6–8} In 2009, Manicaland Province reported 55,707 confirmed cases of malaria but, by 2013, the number of reported cases had more than tripled to 192,730, despite a significant reduction in the national burden of malaria during the same period.^{8,9}

Understanding the local epidemiology of malaria, particularly heterogeneity across time and space, is critical to achieving control and elimination. Remote sensing data and geographic information systems have been used widely to describe spatial and temporal variations of malaria at macro and micro scales.^{10–14} A national-level malaria risk model using district-level, monthly reported cases of malaria from health facilities across Zimbabwe found that annual and seasonal variations in malaria incidence were explained by rainfall, vapor pressure, and temperature.¹⁵ Malaria risk zones have also been described in Masvingo Province, Zimbabwe,

on the basis of eight environmental factors affecting vector reproduction, development, and survival, showing that southern districts in Masvingo Province had the highest risk of malaria.¹⁶ These data, however, rely on passive case finding, and there is a paucity of malaria risk maps and models describing the spatial distribution of malaria in Zimbabwe that are based on active case-finding data.^{15–18}

The aim of this study was to develop a prediction model based on environmental risk factors and to construct seasonal malaria risk maps for Mutasa District, one of the districts with the highest burden of malaria in Zimbabwe. In contrast to previous malaria risk maps and models,^{15,16} spatial and seasonal variation of malaria in relation to environmental factors in Zimbabwe are described at the finer geographic scale of a district. In addition, malaria prevalence data are based on active case detection through household surveys, whereas other risk maps and models in Zimbabwe were based on reported malaria cases available from health facilities.^{15,16} Describing the spatial patterns of malaria transmission and identifying the environmental factors driving spatial and seasonal variation of malaria provide a deeper understanding of local malaria epidemiology and can inform the planning and implementation of malaria control strategies at the spatial scale at which most malaria control programs operate.

METHODS

Study area. This study was conducted in Mutasa District, Manicaland Province, between October 2012 and September 2015. Mutasa District is situated in the northeast of Zimbabwe, bordering the Maniça Province of Mozambique (Figure 1). Mutasa District stretches from 18.20° to 18.58°S latitude and from 32.71° to 33.06°E longitude, and covers an area of 622 km², with an estimated population of 170,000, mostly agricultural laborers. Elevation varies from 600 m in the river valleys to 2,500 m in the inland mountain areas. The average daily temperature is 21.5°C, varying from 24.5°C in November to 16.3°C in July. Transmission of *Plasmodium falciparum*

*Address correspondence to Mufaro Kanyangarara, Department of International Health, Johns Hopkins Bloomberg School of Public Health, Johns Hopkins University, 615 North Wolfe Street, Baltimore, MD 21205. E-mail: mkanyan1@jhu.edu

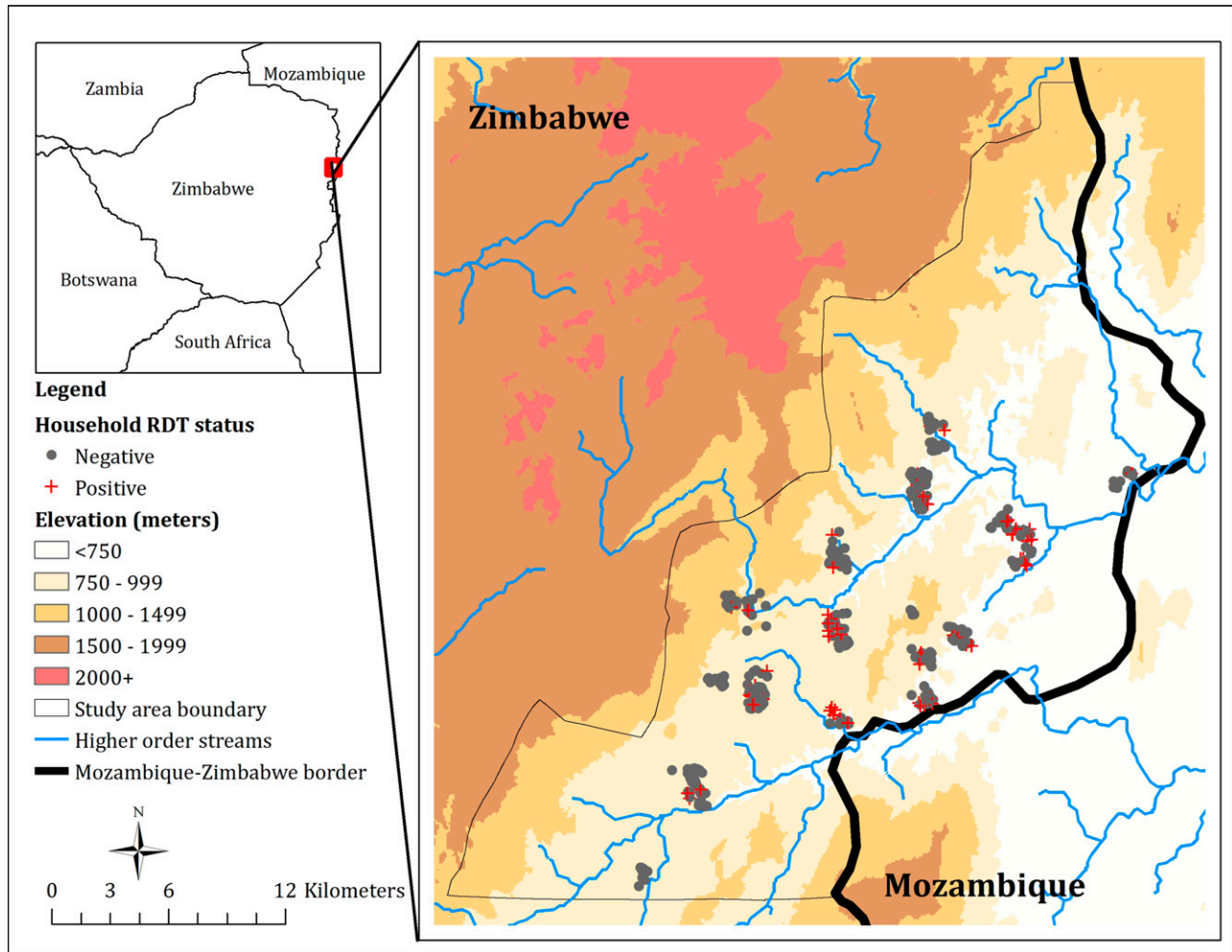


FIGURE 1. Map of Mutasa District, Zimbabwe, indicating positive and negative households.

malaria is highly seasonal, with peaks during the rainy season (November–April).^{15,19} *Anopheles funestus* is the major malaria vector.

Parasitological data. Parasite prevalence was obtained from ongoing community-based surveys in Mutasa District as part of the Southern Africa International Centers of Excellence for Malaria Research (ICEMR). Details of the sampling and study procedures have been described elsewhere.²⁰ In brief, a sampling frame was generated using a high-resolution satellite image of the study area obtained from DigitalGlobe Services, Inc. (Denver, CO).²¹ Grids 1×1 km comprised the sampling frame and were purposefully selected to ensure geographic variation while minimizing logistical challenges. A random sample of households from each of the selected grids was generated, and the latitude and longitude of each selected household were confirmed by trained interviewers using a handheld Global Positioning System. A household was defined as a group of people residing together in one or more domestic structures in the past 2 weeks. All household members, and caregivers in the case of minors, were informed of the study purpose and procedures and were invited to participate. Demographic and socioeconomic information at the individual and household level was obtained using questionnaires administered by research staff to household members and heads of households, respectively. As part of the survey,

participants were asked to provide a fingerprick blood sample that was tested for histidine-rich protein 2 antigen of *P. falciparum* using a rapid diagnostic test (RDT) (SD-Bioline Malaria Antigen P.f; Standard Diagnostics, Inc., Kyonggi, Republic of Korea). RDT-positive participants were offered treatment with artemisinin-based combination therapy in accordance with national policies. Household RDT status, defined as positive for any household having at least one RDT-positive resident, was the outcome of interest.

Environmental data. Using a variety of sources, sets of environmental variables including elevation, slope, aspect, vegetation cover, land use, distances to streams of different categories, distance to the main road, distance to the nearest health facility, distance to the Mozambique border, and household density were compiled and linked to household RDT status. Elevation was extracted from a 90-m, high-resolution Shuttle Radar Topography Mission digital elevation model (DEM).²² DEM-derived raster maps were used to obtain slope (degree of elevation) and aspect (orientation of slope) in degrees for each participating household. The normalized difference vegetation index (NDVI), a proxy for vegetation cover, was derived from a multispectral Landsat-8™ image from July 2014 available from the U.S. Geological Survey Land Processes Distributed Active Archive Center (USGS Earth Resources Observation and Science [EROS] Center,

Sioux Falls, SD). Using bands 4 and 5, corresponding to the red and near-infrared spectral bands, an NDVI raster layer was calculated as: $NDVI = (Band\ 5 - Band\ 4) / (Band\ 5 + Band\ 4)$. Using the same Landsat-8™ image, a land use raster layer was created by performing unsupervised land use classification.²³ Land use classes included: water, impervious, bare land, grass, crop, and forest.

Hydrologic analysis was performed using the DEM to create a stream-network layer, containing attribute information expressing the classifications of streams using Strahler's method.²⁴ In this classification, a stream of order 2 is formed when two streams of order 1 join. Stream classifications ranged from 1 indicating low-volume streams typically present only during the rainy season, to 4 indicating high-volume, year-round streams usually found at lower elevations. The two major rivers in Mutasa District, the Pungwe and Honde, had a stream order of 4. The Euclidean distance from each household to the nearest stream in each of the four classes was calculated in ArcGIS 10.2 (ESRI, Redlands, CA). Similar processes were used to identify the distance from each participating household to the nearest road, health facility, and the Mozambique border. Using the geographic coordinates of all enumerated households in the study area, a measure of household density was computed as the number of structures within 250 m of a participating residence. A binary variable denoting the rainy season (defined as the period between November and April) versus the dry season, was generated based on rainfall data from the Southern Africa ICMR field station in Hauna, a commercial center in Mutasa District. All images and features were projected into Universal Transverse Mercator zone 36S coordinate system to allow the calculation of distances in meters.

Statistical analyses. The outcome of interest was whether a household had at least one member test positive by RDT for malaria parasites. Exploratory data analysis comparing environmental variables between positive and negative households was conducted using χ^2 tests for categorical variables and *t* test for continuous variables. Logistic regression was used to model the probability of household positivity as a function of the environmental covariates. An initial multivariate logistic regression model included all environmental variables found to be significant ($P < 0.1$) in univariate analyses. An indicator variable for the rainy season (November–April) was also considered in the model both as a main effect and as an interaction to allow for effect modification due to season. A manual stepwise variable selection procedure was used and overall model fit examined by the Akaike information criterion (AIC) and Hosmer-Lemeshow goodness of fit test. A *P* value greater than 0.05 for the Hosmer-Lemeshow test statistic and a lower value of AIC indicate a better fitting model. Semivariograms of the standardized residuals from the final logistic regression model residuals were used to assess residual spatial variation.²⁵

Prediction performance of the final multivariate logistic regression model was evaluated as follows. Internal prediction performance of the final model was evaluated using Monte Carlo cross-validation with 1,000 iterations. The total number of households sampled between October 2012 and September 2015 was randomly split; one-third of sampled households were assigned to the test set and the remaining to the training set. The final multivariate logistic regression model was then fit to the training set and predictions made over the test set.

Sensitivity, specificity, and the area under the curve (AUC) of the receiver operating characteristic (ROC) curve were used to assess model performance in both the internal and an external evaluation. The sensitivity was defined as the proportion of true positives the model predicted as being positive, while the specificity was defined as the proportion of true negatives the model classified as being negative. To classify a household as positive or negative, a cutoff was applied to the predicted probabilities. The whole range of cutoffs (0–1) was examined and results were plotted on an ROC curve. A cutoff was chosen to maximize both sensitivity and specificity. After implementing 1,000 iterations of this process redefining new test and training data subsets, the sensitivity and specificity at the optimal cutoff from each iteration was averaged and the corresponding 95% prediction intervals were computed.

External evaluation of the model prediction performance was assessed by fitting the final model to the training set based on data from October 2012 to September 2014 and predicting to the test set comprised of the households enrolled in the most recent 12 months (October 1, 2014 to September 30, 2015). Sensitivity, specificity, and AUC were computed and reported.

The final multivariate logistic regression model built on data from October 2012 to September 2015 was then used to predict and map the probability of household RDT positivity. A fine grid of 100×100 m² cells covering Mutasa District was created within ArcGIS 10.2 and values of environmental determinants were extracted to the centroid of each grid cell. Model predictions and prediction standard errors were generated for each grid cell and stratified by season via the rainy/dry season variable included in the final model.

All spatial data manipulations, processing of environmental data and distance calculations were performed in ArcGIS 10.2. All statistical and spatial statistical analyses were carried out in R statistical software version 3.1.0 (R Core Team, Vienna, Austria).²⁶

Ethical considerations. The institutional review boards of the Johns Hopkins Bloomberg School of Public Health, the Biomedical Research and Training Institute, and the Medical Research Council of Zimbabwe approved this research. Permission was sought from local chiefs for conduct of the study in their area of control and written informed consent was obtained from all adult participants. Consent was obtained from caregivers or legal guardians of minors, with assent for those aged 7–16 years.

RESULTS

Household characteristics. A total of 20,247 structures were identified in Mutasa District from the manual digitization of households. Between October 2012 and September 2015, 483 households participated in the household surveys. The total number of individuals per household varied from one to 25, with the typical family averaging 3.7 household members. Of the 1,774 individuals in the sampled households, 299 (17%) were children younger than 5 years and 983 (55%) were female. One hundred and four individuals representing 69 households tested RDT-positive, giving a malaria prevalence of 104/1,774 (6%) for individuals and 69/483 (14%) for households. Most of the participating households were located in the Honde Valley running through the center of the district (Figure 1). The median elevation of participating households

TABLE 1
Characteristics of 483 sampled households by RDT status in Mutasa District, October 2012–September 2015

Variable	All sampled households	RDT-positive households	RDT-negative households	P value
	N = 483	N = 69	N = 414	
	Median (IQR)	Median (IQR)	Median (IQR)	
Elevation (m)	786 (756–822)	777 (747–802)	787 (757–827)	0.02
Distance to first order streams (m)	618 (398–786)	611 (379–773)	619 (404–786)	0.4
Distance to second order streams (m)	1,281 (922–1,566)	1,439 (1,040–1,704)	1,264 (893–1,548)	0.01
Distance to third order streams (m)	1,703 (623–2,289)	1,637 (637–2,114)	1,727 (623–2,319)	0.6
Distance to fourth order streams (m)	2,088 (1,206–3,783)	2,030 (1,051–3,796)	2,082 (1,365–3,764)	0.6
Distance to nearest health facility (m)	1,617 (581–3,377)	1,891 (889–3,944)	1,600 (571–2,696)	0.1
Distance to main road (m)	1,573 (761–3,098)	1,901 (1,027–4,211)	1,577 (741–3,167)	0.06
Distance to Mozambique border (m)	5,724 (4,457–9,229)	4,852 (2,857–7,102)	6,450 (4,504–9,378)	0.002
NDVI	0.2 (0.2–0.3)	0.2 (0.2–0.3)	0.2 (0.2–0.3)	0.6
Slope of landscape (degree)	1.3 (0.6–2.5)	1.4 (0.7–2.1)	1.3 (0.6–2.5)	0.8
No. of houses within 250-m circular buffer	18 (9–38)	11 (8–25)	19 (9–40)	0.2

IQR = interquartile range; NDVI = normalized difference vegetation index; RDT = rapid diagnostic test.

was 786 m compared with a median elevation of 828 m for all enumerated households. Overall, households with at least one RDT-positive resident tended to be located at lower elevations, further from the main road, closer to the Mozambique border and in more sparsely populated areas (Table 1).

The final multivariate logistic regression model indicated that households sampled during the rainy season were three times more likely to be positive than households sampled in the dry season (adjusted odds ratio [aOR] = 3.17, 95% confidence interval [CI] = 1.78–5.86). Distance to the Mozambique border was strongly associated with household RDT status. Specifically, for every 1,000 m increase in distance from the Mozambique border, the odds of a household having at least one RDT-positive resident decreased 12% (aOR = 0.88, 95% CI = 0.79–0.96). Although the main effect of elevation was not significant (aOR = 1.02, 95% CI = 0.97–1.06, per 10 m increase in elevation), the effect of elevation was modified by season (i.e., significant season by elevation interaction) and hence elevation was retained as a main effect. In the rainy season, for every 10 m increase in elevation, there was a 9% decrease in the household risk of malaria (aOR = 0.91, 95% CI = 0.84–0.97). Households located on east- or southeast-facing slopes were 2.4 times more likely to be positive than households located on other facing slopes (aOR = 2.43, 95% CI = 1.39–4.26). The risk a household had at least one RDT-positive resident increased by 19% for every kilometer increase in distance to the nearest health facility (aOR = 1.19, 95% CI = 1.03–1.37) (Table 2).

The Hosmer-Lemeshow goodness of fit statistic for the final model was 8.2 with a P value of 0.4, indicating the model was a good fit for the data. There was little indication of residual spatial variation (spatial dependence in the regression model residuals) as evidenced by comparing the estimated semivariograms of Pearson standardized residuals from the null model (no included regression covariates) and final model. AIC results showed that the final model offered a better fit than the null intercept model (AIC for null model = 398, AIC for full model = 364).

The Monte Carlo prediction performance evaluation randomly assigned 166 (33%) households to a test set and the remaining 317 (67%) households to a training set. In the training locations, the model had an overall specificity and sensitivity of 89% and 49%, respectively. For the rainy season, the sensitivity and specificity of the model were 61% and 80%, respectively. The model performance during the dry season had better specificity (96%) but far worse sensitivity (37%). When the model was evaluated prospectively by holding out the last 12 months of data (external evaluation), the specificity was higher than the sensitivity overall and in both seasons.

The risk map for the dry season was characterized by low risk across the entire study area, with pockets of elevated risk scattered along the northern, western, and southeastern peripheries of the study area (Figure 2A). In contrast, the risk map for the rainy season depicted relatively increased risk of finding a positive household (> 50%) in the eastern part of the study

TABLE 2

Univariate and multivariable logistic regression models of environmental factors associated with household RDT status in Mutasa District, October 2012–September 2015

	Univariate models			Multivariable model		
	OR	95% CI	P value	aOR	95% CI	P value
Rainy season	2.70	1.58–4.75	< 0.001	3.17	1.78–5.86	< 0.001
Distance to Mozambique border (per km)	0.87	0.80–0.95	0.002	0.87	0.79–0.96	0.007
Elevation (per 10 m)	0.97	0.93–1.00	0.06	1.02	0.97–1.06	0.4
Distance to nearest health facility (per km)	1.08	0.96–1.22	0.2	1.19	1.03–1.37	0.02
South- or southeast-facing slope	1.92	1.14–3.21	0.01	2.42	1.38–4.26	0.002
Interaction: elevation (per 10 m) and rainy season	0.91	0.84–0.97	0.006	0.91	0.84–0.97	0.009
Distance to second order stream (per km)	1.70	1.09–2.63	0.02	–	–	–
Number of houses within 250-m circular buffer	0.98	0.94–1.01	0.2	–	–	–
Distance to main road (per km)	1.11	0.97–1.25	0.1	–	–	–

aOR = adjusted odds ratio; CI = confidence interval; OR = odds ratio; RDT = rapid diagnostic test.

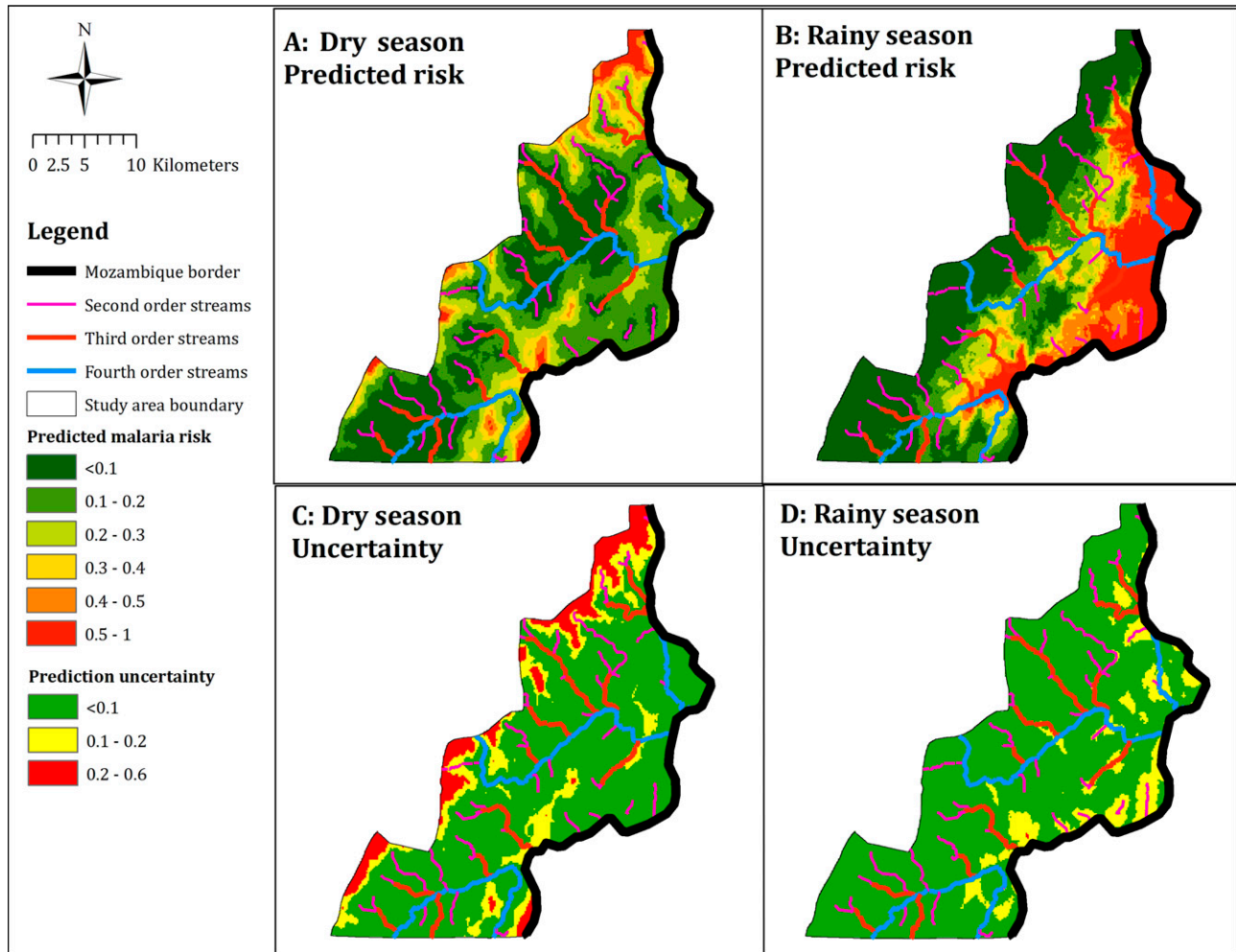


FIGURE 2. Categorical maps of predicted household malaria risk and uncertainty by season for Mutasa District, October 2012–September 2015.

area along the Mozambique border. There was a gradient east to west with a decline in the predicted risk (Figure 2B).

Importantly, a high predicted risk may not imply a high probability of finding a positive household, depending on the precision of the estimate. Examination of the maps of prediction accuracy indicated that the prediction uncertainty was higher in the dry season than in the rainy season (Figure 2C and 2D). For the rainy season, the prediction uncertainty did not exceed 0.1 across most of the study area. However, there were areas with prediction uncertainty in the range of 0.1–0.2 eastwards along the Mozambique border. For the dry season, prediction uncertainty ranged as high as 0.6, with areas scattered along the northern, western, and southeastern peripheries of the study area having the highest uncertainty. Comparing the prediction maps to the corresponding maps of uncertainty for both seasons showed that prediction uncertainty was high at locations where the predictions themselves were high.

DISCUSSION

The application of high-resolution remote sensing data and geostatistics to develop seasonal malaria risk maps at a fine spatial resolution may be crucial to achieving the goal of

malaria elimination. This study used active surveillance data collected prospectively over a period covering high (rainy season) and low (dry season) transmission seasons in a region of resurgent malaria in eastern Zimbabwe. The study revealed heterogeneity of malaria risk over a small geographic area and identified important environmental determinants of the observed spatial pattern of malaria risk. Using a geostatistical approach, the model predicted household malaria risk and allowed for the estimation of uncertainty in predictions. The resulting maps predicted elevated risk during the rainy season, particularly in low-lying areas bordering with Mozambique. In contrast, the risk of malaria was low across the study area during the dry season with foci of malaria scattered along the northern, western, and southeastern peripheries of the study area. The predicted risk maps provide an empirical basis for identifying priority areas for malaria interventions.

The environmental factors found to be related to malaria risk are consistent with previous data on the epidemiology of malaria and vector biology in Zimbabwe. Environmental factors previously identified as driving malaria transmission in the country include season, elevation, rainfall, temperature, and vapor pressure.^{1,15,17,27} The model predicted higher risk of malaria among households sampled in the rainy season, located near the Mozambique border and further from health

facilities. In addition, elevation limited malaria transmission during the rainy season. Previous research in Zimbabwe suggested that malaria transmission does not typically occur at elevations exceeding 1,200 m.¹ Although the range of elevations for enumerated households was between 607 and 1,514 m, for sampled households, the range was limited to between 639 and 1,234 m. The limited range of elevation in the sampled households may be a result of logistical challenges reaching areas at higher elevations. Consequently, differences in malaria risk during the dry season related to elevation may have been masked by the underrepresentation of households at higher elevations.

The study identified proximity to the Mozambique border as an important driver of malaria transmission, even after adjustment for elevation. The border areas of countries with neighbors with a higher burden of malaria often have higher malaria transmission as a result of cross-border movement. In Mpumalanga Province, South Africa, which borders more southerly provinces of Mozambique (Gaza and Maputo), a map of average malaria incidences showed a greater risk of malaria among individuals living within 5 km of the Mozambican border compared with other inhabitants.²⁸ A receptive risk map for malaria in Namibia found that the highest receptive risks of malaria transmission were along the borders with Angola and Zambia.²⁹ In this study, a gradient of malaria risk was identified during the rainy season: compared with households closer to the border with Mozambique, households farther away had a lower risk of malaria. These findings emphasize the need for regional collaborations to control malaria.

The high-resolution risk maps present a new cartographic resource describing important seasonal and spatial heterogeneities in malaria transmission in Zimbabwe. The predicted risk map for the rainy season showed that malaria risk increases from west to east of the study area. In contrast, during the dry season, much of the study area had a low risk but there were foci of malaria transmission scattered across the district. The risk map for the dry season produced a weaker fitting model than for the rainy season, in part, attributable to fewer cases identified during the dry season. In addition, areas predicted to have elevated risk carried higher levels of prediction uncertainty, underscoring the need to acknowledge prediction uncertainties when interpreting malaria risk maps for disease control. Understanding the prediction, uncertainty may help in the identification of areas in need of additional sampling to develop a more accurate map of the seasonal and spatial variation of malaria risk.

This study has several important limitations. First, the uneven geographical distribution of study household data may limit the power to identify spatial heterogeneity, particularly in the peripheries of the study area where prediction uncertainty was highest. Spatial predictions are more precise and accurate in areas closer to sampled households. Although there is less confidence about predictions in parts of the study area, the analytical approach quantified the prediction uncertainty. The smoothed maps of prediction uncertainty can be harnessed to prioritize future data collection in parts of the study area exhibiting higher uncertainty. Second, the analytical approach included only explanatory variables that were available or could be computed for any geographic location within the study area. Consequently, individual-level data and household characteristics available through questionnaires administered during ongoing surveys were not included in the

models. It is likely that other factors related to age, socioeconomic status, occupation, travel history, and use of preventative measures may influence the observed distribution of malaria in Mutasa District. Finally, the outcome, household RDT status fails to account for the frequency or proportion of RDT-positive residents within a household. For example, based on the current approach, a household of five with one RDT-positive resident and a household of five with all five RDT-positive residents were considered RDT-positive households. From a programmatic perspective, identifying any household exposure regardless of intensity is important as vector control measures such as IRS occur at the household level.

Characterizing the heterogeneity in the spatial distribution of malaria in this small geographic area should enhance the understanding of the local malaria epidemiology and identified areas of high risk where additional control efforts should be conducted as a strategic priority to reduce malaria transmission. The models and maps were aimed at local policy and decision-making and these results will help in the development of long-term and sustainable strategies for malaria control in Mutasa District, Zimbabwe.

Received November 30, 2015. Accepted for publication January 31, 2016.

Published online April 25, 2016.

Acknowledgments: We would like to thank the field team for their assistance in data collection and the community in Mutasa District for participating in this study.

Financial support: This work was supported by the Division of Microbiology and Infectious Diseases, National Institutes of Allergy and Infectious Diseases, National Institutes of Health as part of the International Centers of Excellence for Malaria Research (U19 AI089680).

Authors' addresses: Mufaro Kanyangarara and Luke C. Mullany, Department of International Health, Johns Hopkins Bloomberg School of Public Health, Johns Hopkins University, Baltimore, MD, E-mails: mkanyan1@jhu.edu and lmullany@jhu.edu. Edmore Mamini, Sungano Mharakurwa, Shungu Munyati, and Peter R. Mason, Biomedical Research and Training Institute, Harare, Zimbabwe, E-mails: edmoremamini@gmail.com, smharak1@jhu.edu, smunyati@brti.co.zw, and pmason@brti.co.zw. Lovemore Gwanzura, Department of Medical Laboratory Sciences, College of Health Sciences, University of Zimbabwe, Harare, Zimbabwe, E-mail: gwanzura@mweb.co.zw. Tamaki Kobayashi, Timothy Shields, Frank C. Curriero, and William J. Moss, Department of Epidemiology, Johns Hopkins Bloomberg School of Public Health, Johns Hopkins University, Baltimore, MD, E-mails: tkobaya2@jhu.edu, tshield2@jhu.edu, fcurriero@jhu.edu, and wmoss1@jhu.edu. Susan Mutambu, National Institute of Health Research, Harare, Zimbabwe, E-mail: mutambusl@gmail.com.

REFERENCES

1. Taylor P, Mutambu SL, 1986. A review of the malaria situation in Zimbabwe with special reference to the period 1972–1981. *Trans R Soc Trop Med Hyg* 80: 12–19.
2. Mharakurwa S, Thuma PE, Norris DE, Mulenga M, Chalwe V, Chipeta J, Munyati S, Mutambu S, Mason PR, 2012. Malaria epidemiology and control in southern Africa. *Acta Trop* 121: 202–206.
3. Mharakurwa S, Mutambu SL, Mudyiradima R, Chimbadzwa T, Chandiwana SK, Day KP, 2004. Association of house spraying with suppressed levels of drug resistance in Zimbabwe. *Malar J* 3: 35.
4. Munhenga G, Masendu HT, Brooke BD, Hunt RH, Koekemoer LK, 2008. Pyrethroid resistance in the major malaria vector *Anopheles arabiensis* from Gwave, a malaria-endemic area in Zimbabwe. *Malar J* 7: 247.
5. Choi KS, Christian R, Nardini L, Wood OR, Agubuzo E, Muleba M, Munyati S, Makuwaza A, Koekemoer LL, Brooke

- BD, Hunt RH, Coetzee M, 2014. Insecticide resistance and role in malaria transmission of *Anopheles funestus* populations from Zambia and Zimbabwe. *Parasit Vectors* 7: 464.
6. Lewis R, Hamade P, 2008. *Roll Back Malaria: Country Needs Assessment*. Zimbabwe Report. Harare, Zimbabwe: Malaria Consortium.
 7. Zimbabwe Ministry of Health and Child Welfare, 2012. *Zimbabwe National Health Profile, 2012*. Harare, Zimbabwe: Zimbabwe Ministry of Health and Child Welfare.
 8. Zimbabwe Ministry of Health and Child Welfare, 2009. *Zimbabwe National Health Profile, 2009*. Harare, Zimbabwe: Zimbabwe Ministry of Health and Child Welfare.
 9. President's Malaria Initiative, 2015. *Zimbabwe Malaria Operational Plan FY 2015*. Washington, DC: President's Malaria Initiative.
 10. Moss WJ, Hamapumbu H, Kobayashi T, Shields T, Kamanga A, Clennon J, Mharakurwa S, Thuma PE, Glass G, 2011. Use of remote sensing to identify spatial risk factors for malaria in a region of declining transmission: a cross-sectional and longitudinal community survey. *Malar J* 10: 163.
 11. Alemu A, Abebe G, Tsegaye W, Golassa L, 2011. Climatic variables and malaria transmission dynamics in Jimma town, south west Ethiopia. *Parasit Vectors* 4: 30.
 12. Eisele TP, Keating J, Swalm C, Mbogo CM, Githeko AK, Regens JL, Githure JI, Andrews L, Beier JC, 2003. Linking field-based ecological data with remotely sensed data using a geographic information system in two malaria endemic urban areas of Kenya. *Malar J* 2: 44.
 13. Noor AM, ElMardi KA, Abdelgader TM, Patil AP, Amine AA, Bakhiet S, Mukhtar MM, Snow RW, 2012. Malaria risk mapping for control in the Republic of Sudan. *Am J Trop Med Hyg* 87: 1012–1021.
 14. Pinchoff J, Chaponda M, Shields T, Lupiya J, Kobayashi T, Mulenga M, Moss WJ, Curriero FC; Southern Africa International Centers of Excellence for Malaria Research, 2015. Predictive malaria risk and uncertainty mapping in Nchelenge District, Zambia: evidence of widespread, persistent risk and implications for targeted interventions. *Am J Trop Med Hyg* 93: 1260–1267.
 15. Mabaso MLH, Vounatsou P, Midzi S, Da Silva J, Smith T, 2006. Spatio-temporal analysis of the role of climate in inter-annual variation of malaria incidence in Zimbabwe. *Int J Health Geogr* 5: 20.
 16. Chikodzi D, 2013. Spatial modelling of malaria risk zones using environmental, anthropogenic variables and geographical information systems techniques. *J Geosci Geomatics*. 1: 8–14.
 17. Ebi KL, Hartman J, Chan N, McConnell J, Schlesinger M, Weyant J, 2005. Climate suitability for stable malaria transmission in Zimbabwe under different climate change scenarios. *Clim Change* 73: 375–393.
 18. Ohemeng FD, Mukherjee F, 2015. Modelling the spatial distribution of the *Anopheles* mosquito for malaria risk zoning using remote sensing and GIS: a case study in the Zambezi Basin, Zimbabwe. *Int J Appl Geospatial Res* 6: 7–20.
 19. Mabaso MLH, Craig M, Vounatsou P, Smith T, 2005. Towards empirical description of malaria seasonality in southern Africa: the example of Zimbabwe. *Trop Med Int Health* 10: 909–918.
 20. Moss WJ, Norris DE, Mharakurwa S, Scott A, Mulenga M, Mason PR, Chipeta J, Thuma PE, 2012. Challenges and prospects for malaria elimination in the southern Africa region. *Acta Trop* 121: 207–211.
 21. Lowther SA, Curriero FC, Shields T, Ahmed S, Monze M, Moss WJ, 2009. Feasibility of satellite image-based sampling for a health survey among urban townships of Lusaka, Zambia. *Trop Med Int Health* 14: 70–78.
 22. Shuttle Radar Topography Mission NASA. (SRTM). *SRTM Digital Elevation Model*. Available at: <http://www2.jpl.nasa.gov/srtm/>. Accessed October 1, 2015.
 23. Anderson JR, 1976. *A Land Use and Land Cover Classification System for Use with Remote Sensor Data*, Vol 964. Arlington, VA: U.S. Government Printing Office.
 24. Strahler AN, 1952. Hypsometric (area-altitude) analysis of erosional topography. *Geol Soc Am Bull* 63: 1117–1142.
 25. Cressie NAC, Cassie NA, 1993. *Statistics for Spatial Data*, Vol 900. New York, NY: Wiley.
 26. R Development Core Team, 2013. *R: A language and Environment for Statistical Computing*. Vienna, Austria: R Foundation for Statistical Computing.
 27. Freeman T, Bradley M, 1996. Temperature is predictive of severe malaria years in Zimbabwe. *Trans R Soc Trop Med Hyg* 90: 232.
 28. Booman M, Durrheim DN, La Grange K, Martin C, Mabuza AM, Zitha A, Mbokazi FM, Fraser C, Sharp BL, 2000. Using a geographical information system to plan a malaria control programme in South Africa. *Bull World Health Organ* 78: 1438–1444.
 29. Noor AM, Uusiku P, Kamwi RN, Katokele S, Ntomwa B, Alegana VA, Snow RW, 2013. The receptive versus current risks of *Plasmodium falciparum* transmission in northern Namibia: implications for elimination. *BMC Infect Dis* 13: 184.